Available online at www.sciencedirect.com
SCIENCE DIRECT®
PHYSICS LETTERS B
ELSEVIER
Physics Letters B 553 (2003) 167–178
www.elsevier.com/locate/npe

Charmonia and Drell–Yan production in proton–nucleus collisions at the CERN SPS

NA50 Collaboration

B. Alessandro [k], C. Alexa [d], R. Arnaldi [k], M. Atayan [m], C. Baglin [b], S. Beolè [k], V. Boldea [d], P. Bordalo [g,1], S.R. Borenstein [j,2], G. Borges [g], A. Bussière [b], L. Capelli [l], C. Castanier [c], J. Castor [c], B. Chaurand [j], B. Cheynis [l], E. Chiavassa [k], C. Cicalò [e], T. Claudino [g], M.P. Comets [i], N. Constans [j], S. Constantinescu [d], P. Cortese [a], J. Cruz [g], A. De Falco [e], N. De Marco [k], G. Dellacasa [a], A. Devaux [c], S. Dita [d], O. Drapier [j], L. Ducroux [l], B. Espagnon [c], J. Fargeix [c], P. Force [c], M. Gallio [k], Y.K. Gavrilov [h], C. Gerschel [i], P. Giubellino [k,3], M.B. Golubeva [h], M. Gonin [j], A.A. Grigorian [m], S. Grigorian [m], J.Y. Grossiord [l], F.F. Guber [h], A. Guichard [l], H. Gulkanyan [m], R. Hakobyan [m], M. Idzik [k,4], D. Jouan [i], T.L. Karavitcheva [h], L. Kluberg [j], A.B. Kurepin [h], Y. Le Bornec [i], C. Lourenço [f], P. Macciotta [e], M. Mac Cormick [i], A. Marzari-Chiesa [k], M. Masera [k,3], A. Masoni [e], M. Monteno [k], A. Musso [k], P. Petiau [j], A. Piccotti [k], J.R. Pizzi [l], W. Prado da Silva [k,5], F. Prino [a], G. Puddu [e], C. Quintans [g], L. Ramello [a], S. Ramos [g,1], P. Rato Mendes [g], L. Riccati [k], A. Romana [j], H. Santos [g], P. Saturnini [c], E. Scalas [a], E. Scomparin [k], S. Serci [e], R. Shahoyan [g,6], F. Sigaudo [k], M. Sitta [a], P. Sonderegger [f,2], X. Tarrago [i], N.S. Topilskaya [h], G.L. Usai [e,3], E. Vercellin [k], L. Villatte [i], N. Willis [i]

[a] *Universitá del Piemonte Orientale, Alessandria and INFN Torino, Italy*
[b] *LAPP, CNRS-IN2P3, Annecy-le-Vieux, France*
[c] *LPC, Université Blaise Pascal and CNRS-IN2P3, Aubière, France*
[d] *IFA, Bucharest, Romania*
[e] *Università di Cagliari/INFN, Cagliari, Italy*
[f] *CERN, Geneva, Switzerland*
[g] *LIP, Lisbon, Portugal*
[h] *INR, Moscow, Russia*
[i] *IPN, Université de Paris-Sud and CNRS-IN2P3, Orsay, France*
[j] *LPNHE, Ecole Polytechnique and CNRS-IN2P3, Palaiseau, France*
[k] *Università di Torino/INFN, Torino, Italy*
[l] *IPN, Université Claude Bernard Lyon-I and CNRS-IN2P3, Villeurbanne, France*
[m] *YerPhI, Yerevan, Armenia*

Received 9 December 2002; accepted 19 December 2002

Editor: L. Montanet

0370-2693/02/$ – see front matter
doi:10.1016/S0370-2693(02)03265-3

Abstract

Charmonium production in p–A collisions is a unique tool for the study of the interaction of bound $c\bar{c}$ states in nuclear matter. It can provide details on the basic features of the resonance formation mechanism and, in particular, on its non-perturbative aspects. In this Letter, we present an experimental study of charmonia and Drell–Yan production in proton–nucleus collisions at 450 GeV/c. The results are analyzed in the framework of the Glauber model and lead to the values of the nuclear absorption cross-section $\sigma_{pA}^{\mathrm{abs}}$ for J/ψ and ψ'. Then, we compare the J/ψ absorption in proton–nucleus and sulphur–uranium interactions, using NA38 data. We obtain that, for the J/ψ, $\sigma_{pA}^{\mathrm{abs}}$ and $\sigma_{\mathrm{SU}}^{\mathrm{abs}}$ are compatible, showing that no sizeable additional suppression mechanism is present in S–U collisions, and confirming that the anomalous J/ψ suppression only sets in for Pb–Pb interactions.

1. Introduction

The study of charmonia production in proton–nucleus collisions allows the investigation of the absorption mechanisms of the $c\bar{c}$ state in its path across the nucleus. A considerable theoretical effort has been carried out in the past few years [1] in order to interpret the experimental results available from fixed target experiments at CERN and FNAL energies ($\sqrt{s} \sim 20$–40 GeV) [2–5]. The results show that the perturbatively produced $c\bar{c}$ pair neutralizes its colour on a timescale which, depending on the kinematical variables of the pair, is of the same order of magnitude, or even larger, than the time needed for the heavy-quark pair to escape the nuclear environment. However, a satisfactory quantitative description of the time evolution of the $c\bar{c}$ pair until it becomes a colour-neutral charmonium resonance is not available up to now. Therefore, new data, relative to charmonium production, can help in constraining the model parameters and, more generally, in testing the validity of the approach used up to now in the interpretation of p–A data.

Furthermore, the study of the J/ψ in the SPS energy range is interesting as a signature of QGP formation. A sizeable suppression of the J/ψ yield has been measured in Pb–Pb collisions by the NA50 Collaboration [7–9], as expected if a phase transition to deconfined partonic matter occurs in those interactions [6]. In particular, analyzing the high statistics J/ψ data from the NA38 and NA51 experiments, relative to p–p, p–d and S–U collisions [10], it has been shown that the observed yield can be reasonably explained in terms of a suppression of this meson exclusively due to hadronic processes. On the contrary, in Pb–Pb collisions there is an extra ("anomalous") suppression that is difficult to explain with conventional mechanisms.

However, high statistics p–A data on nuclei heavier than deuterium, in particular for what concerns Drell–Yan and ψ' events, were not available up to now within the wide systematic studies performed by the NA38/NA50/NA51 experiments [10]. From a comparison of the yields in p–A and S–U collisions one can in principle disentangle the different sources of hadronic J/ψ suppression: the nuclear absorption, present in both p–A and S–U interactions, and the interaction of the J/ψ with the generated secondary particles (comovers), expected to play a sizeable role only in nucleus–nucleus collisions. The size of the second effect is up to now poorly known.

To investigate these points, the NA50 Collaboration has carried out an experimental study of charmonia production with a 450 GeV/c incident proton beam. The charmonia resonances J/ψ and ψ' have been identified through their decay into muon pairs. Various nuclear targets, namely Be, Al, Cu, Ag and W have been used, and for each target about 10^5 J/ψ events have been collected. Each event sample contains also ~ 500 high mass dimuon events ($m_{\mu\mu} > 5$ GeV/c^2), due to the Drell–Yan process, that have been used as a reference in the study of the J/ψ suppression. Preliminary results on these data have been reported

E-mail address: scompar@to.infn.it (E. Scomparin).

[1] Also at IST, Universidade Técnica de Lisboa, Lisbon, Portugal.

[2] On leave of absence from York College CUNY, USA.

[3] Also at CERN, Geneva, Switzerland.

[4] Also at Faculty of Physics and Nuclear Techniques, University of Mining and Metallurgy, Cracow, Poland.

[5] Now at UERJ, Rio de Janeiro, Brazil.

[6] On leave of absence of YerPhI, Yerevan, Armenia.

elsewhere [11–13]. In this Letter, we present the final results on charmonia and Drell–Yan cross-sections, and analyze them in the framework of the Glauber model. We extract in this way the values of the charmonia absorption cross-section in the nuclear medium. Then, with the same model, we re-analyze the NA38 S–U data and compare the corresponding J/ψ absorption cross-section to the one calculated in p–A.

2. Experimental set-up, data reduction and analysis

The p–A data analyzed in this Letter have been taken with the standard NA50 dimuon spectrometer, which, in its heavy-ion set-up, has been described in detail in Ref. [14]. For proton running, the set-up only differs in the target region, where a passive target has been used, and in the detectors used for the luminosity measurement. In particular, the beam intensity was monitored by a set of three argon ionisation chambers put along the beam path. These detectors have been calibrated at low intensity and their linearity has been checked up to 10^{10} proton/s. Furthermore, the stability of the beam impact point has been monitored by means of three scintillator telescopes, positioned at 90 degrees with respect to the beam axis, which measure a small fraction of the secondary particles produced in the target, integrated over the burst.

The data have been collected with a primary proton beam from the CERN SPS at 450 GeV incident energy. The beam intensity was around 2×10^8 protons/s. At this intensity, the event pile-up in the muon spectrometer is negligible, the dimuon trigger rate is of the order of 20 Hz and there is practically no dead time. Five nuclear targets have been used: Be, Al, Cu, Ag and W with thicknesses ranging from $0.3\,\lambda_I$ (Al) to $0.5\,\lambda_I$ (Ag). About 10^6 dimuon events have been collected for each target, and analyzed with the standard NA50 reconstruction program [14]. For about 60% of the triggers, it is possible to fully reconstruct two muons in the spectrometer. Further quality cuts lower the number of events retained for the analysis to about 35% of the initial sample. Namely we require that the reconstructed trajectories of the two tracks do not intercept the iron yokes of the spectrometer's air-core magnet [15] and that the two muons point to the target. For the accepted events, the rapidity selection $-0.4 < y_{\rm cm} < 0.6$ and the angular selection $-0.5 < \cos\theta_{\rm CS} < 0.5$, corresponding to the kinematical window of the spectrometer's acceptance, have been applied to reconstructed muon pairs. The angle $\theta_{\rm CS}$ is the polar angle of the μ^+ relative to the bisector of the angle between the momenta $\vec{p}_{\rm beam}$ and $-\vec{p}_{\rm target}$ in the rest frame of the dimuon (the so-called Collins–Soper reference frame). The trigger efficiency $\epsilon_{\rm trig}$ has been measured with a dedicated system of two scintillator hodoscopes, and ranges from 86 to 90%. The dimuon reconstruction efficiency $\epsilon_{\mu\mu}$ is directly related to the efficiency of the MWPCs of the muon spectrometer. The calculated values slightly depend on the beam intensity and are larger than 97%.

In Fig. 1 we show the p–Be and p–W dimuon invariant mass spectra in the region $2 < m_{\mu\mu} < 7$ GeV/c^2, after data reduction. The dimuon sources in this region are the charmonia resonances (J/ψ and ψ'), the Drell–Yan process (DY) and the semi-leptonic decays of charmed hadron pairs ($D\overline{D}$). A contribution mainly due to the uncorrelated decays of pions and kaons (combinatorial background) is also present. Its size can be estimated starting from the measured $\mu^+\mu^+$ and $\mu^-\mu^-$ invariant mass spectra, according to the formula:

$$\frac{dN^{+-}_{\rm bck}}{dm} = 2R_{\rm bck}\sqrt{\frac{dN^{++}}{dm}\frac{dN^{--}}{dm}}\,\frac{A^{+-}}{\sqrt{A^{++}A^{--}}}, \qquad (1)$$

where A^{+-}, A^{++}, A^{--} are the acceptances for opposite-sign and like-sign dimuons. An offline cut is applied to the data in order to ensure that the acceptance of the spectrometer is independent of the charge of the detected muons; consequently we get $A^{+-}/\sqrt{A^{++}A^{--}} = 1$. The factor $R_{\rm bck}$ accounts for charge correlation effects connected with charge conservation in the reaction. It has been estimated through a Monte Carlo simulation based on VENUS 4.12, described in detail in Ref. [16], and cross-checked with an experimental measurement performed for p–W collisions [17]. The $R_{\rm bck}$ values used in this analysis range from 1.09 to 1.14, depending on beam intensity and target. In any case, in the mass region $m_{\mu\mu} > 2.9$ GeV/c^2, corresponding to charmonia resonances, the contribution of the combinatorial background is almost negligible, amounting to less than 0.2% of the total dimuon yield.

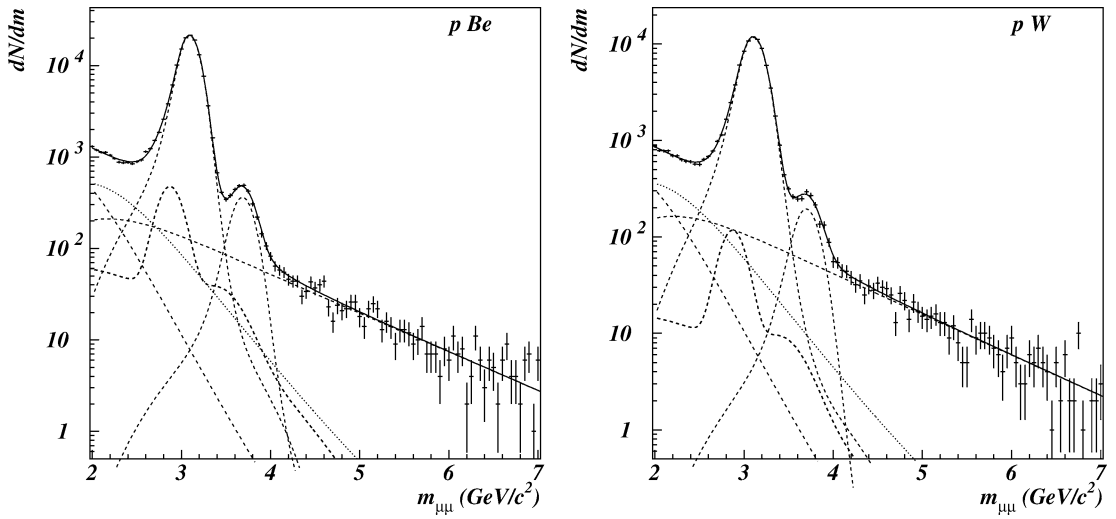

Fig. 1. The p–Be and p–W invariant mass spectra, after data reduction. The continuous line represents the result of the fit. The dashed lines correspond to the DY, J/ψ and ψ' contributions, the dotted line to the $D\overline{D}$ process, while the dashed-dotted line is the combinatorial background. The contribution of the target-out events is shown as a thick dashed line.

Table 1
Number of J/ψ, ψ', Drell–Yan events, not corrected for acceptance, and χ^2/ndf of the fits to the p–A data samples. The Drell–Yan statistics corresponds to the mass interval $2.9 < m_{\mu\mu} < 4.5$ GeV/c^2

	p–Be	p–Al	p–Cu	p–Ag	p–W
J/ψ	124754 ± 391	100703 ± 397	130582 ± 423	132136 ± 366	78156 ± 287
ψ'	2429 ± 69	2016 ± 63	2509 ± 75	2458 ± 73	1392 ± 58
Drell–Yan	2445 ± 78	2184 ± 72	2726 ± 82	3179 ± 86	1950 ± 67
χ^2/ndf	1.30	1.05	1.45	1.14	1.05

Having fixed the contribution of the combinatorial background, the number of J/ψ, ψ', DY and $D\overline{D}$ events has been estimated by means of a fit to the mass region $2 < m_{\mu\mu} < 7$ GeV/c^2, following the standard NA50 procedure [16]. The shapes of the mass distributions for the various processes have been evaluated by means of a Monte Carlo simulation, using the event generator PYTHIA 5.7 [18], with the MRS (A) low Q^2 $\overline{\text{MS}}$ set of parton distribution functions [19], $m_c = 1.35$ GeV/c^2 and $\langle k_T^2 \rangle = 0.8$ (GeV/c)^2. The calculated mass distributions are not very sensitive to the specific values of these quantities. The relative normalization of the dimuon sources are free parameters in the fit. All the mass spectra are satisfactorily reproduced by a superposition of known sources, with χ^2/ndf ranging from 1.10 to 1.46 (see Fig. 1). The contribution of the off-target interactions has been estimated with dedicated target-out data taking periods and taken into account in the fits. The results have been found to be stable within less than 1% when the starting point for the fit is chosen anywhere in the mass region between 1.8 and 2.6 GeV/c^2. Finally, to check the influence of the open-charm contribution on the evaluation of the J/ψ and Drell–Yan yields, we have performed a set of fits in the mass region $m_{\mu\mu} > 2.9$ GeV/c^2, completely neglecting the open-charm component. The only notable effect is a small systematic increase, by about 2%, in the estimate of the Drell–Yan yield.

The number of J/ψ, ψ' and Drell–Yan dimuon events for each target, together with the χ^2 of the fits, are summarized in Table 1. For Drell–Yan, we show the number of events in the mass region $2.9 < m_{\mu\mu} < 4.5$ GeV/c^2. The acceptances A_i of our apparatus for the studied processes ($i = J/\psi$, ψ', DY) have been calculated via Monte Carlo, as the ratio between the number of reconstructed and generated events in the

kinematical domain defined by $-0.4 < y_{\rm cm} < 0.6$ and $-0.5 < \cos\theta_{\rm CS} < 0.5$. We get $A_{J/\psi} = 14.0\%$, $A_{\psi'} = 16.4\%$ and $A_{\rm DY} = 13.9\%$.

3. Results

In the NA50 kinematical domain, charmonia production occurs essentially through hard gluon–gluon scattering. Therefore the production cross-sections, in absence of nuclear effects, are expected to scale with the number of nucleon–nucleon collisions, which for p–A interactions is proportional to the target mass number A. Such a scaling can be investigated by considering the production cross-section per nucleon–nucleon collision, expressed through the ratios $B_{\mu\mu}\sigma_{J/\psi}/A$ and $B'_{\mu\mu}\sigma_{\psi'}/A$, where $B_{\mu\mu}$ and $B'_{\mu\mu}$ are the charmonia branching ratios into muon pairs. In Fig. 2 and Table 2 we show our results for these quantities. The quoted systematic errors include a 3% uncertainty on the estimation of the absolute proton flux, due to relative instabilities in the response of the argon counters during data taking, and a further contribution due to short range fluctuations of the trigger efficiency, whose size ranges from 1.5 to 3%. A 1% and a 2% error on the measurement of $\epsilon_{\mu\mu}$ and $\epsilon_{\rm trig}$, respectively, is also taken into account. For the J/ψ, we find that the systematic uncertainty is the only sizeable contribution to the calculated errors, while for the ψ' statistical and systematical errors are roughly of the same magnitude. For both resonances, the cross-section per nucleon–nucleon collision significantly decreases with A.

In Fig. 3 we present the Drell–Yan cross-section per nucleon–nucleon collision $\sigma_{\rm DY}/A$, integrated in the mass interval $2.9 < m_{\mu\mu} < 4.5$ GeV/c^2, corrected for the isospin dependence. For a given mass number A, the corrected value is obtained through the relation:

$$\sigma_{\rm DY}^{pA} = \sigma_{\rm DY,meas}^{pA} \frac{A\sigma_{\rm DY,calc}^{pp}}{\sigma_{\rm DY,calc}^{pA}} \tag{2}$$

where $\sigma_{\rm DY,calc}^{pp}$ and $\sigma_{\rm DY,calc}^{pA}$ have been calculated at leading order, using the MRS (A) low Q^2 $\overline{\rm MS}$ set of parton distribution functions. The isospin-corrected cross-sections are equivalent to the Drell–Yan cross-sections that would have been measured if the target nuclei were made of protons only. Their values, as well as the correction factors, are listed in Table 3. We

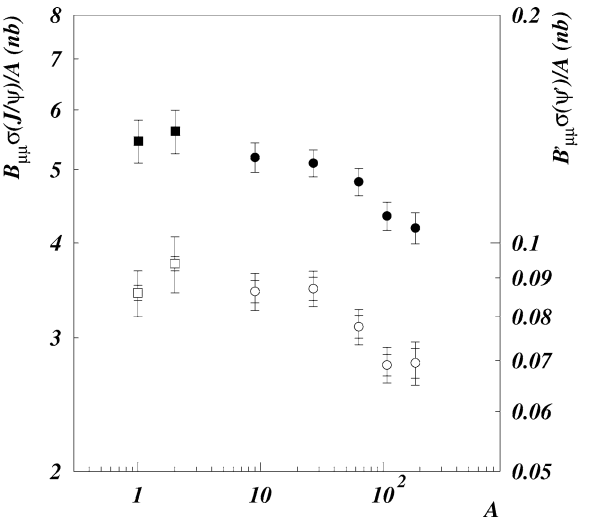

Fig. 2. The J/ψ (closed circles) and ψ' (open circles) cross-sections, divided by the mass number A, for p–A collisions. For the ψ', we plot both statistical (inner bars) and statistical plus systematical errors (outer bars). For the J/ψ, statistical errors are negligible and we only plot systematical errors. The squares represent the NA51 data on p–p and p–d collisions at 450 GeV.

Table 2
The J/ψ and ψ' cross-sections per nucleon–nucleon collision. We quote the statistical and systematical errors separately. NA51 results on p–p and p–d collisions [24] are also included

	$B_{\mu\mu}\sigma_{J/\psi}/A$ (nb/A)	$B'_{\mu\mu}\sigma_{\psi'}/A$ (pb/A)
p–Be	5.19 ± 0.02 (stat.) ± 0.23 (syst.)	86.4 ± 2.9 (stat.) ± 3.9 (syst.)
p–Al	5.10 ± 0.02 (stat.) ± 0.21 (syst.)	87.2 ± 3.1 (stat.) ± 3.6 (syst.)
p–Cu	4.82 ± 0.01 (stat.) ± 0.20 (syst.)	78.6 ± 2.6 (stat.) ± 3.2 (syst.)
p–Ag	4.34 ± 0.01 (stat.) ± 0.19 (syst.)	69.1 ± 2.3 (stat.) ± 3.0 (syst.)
p–W	4.19 ± 0.02 (stat.) ± 0.20 (syst.)	69.5 ± 3.2 (stat.) ± 3.3 (syst.)
p–p (NA51)	5.50 ± 0.01 (stat.) ± 0.36 (syst.)	86 ± 2 (stat.) ± 6 (syst.)
p–d (NA51)	5.62 ± 0.01 (stat.) ± 0.37 (syst.)	94 ± 2 (stat.) ± 7 (syst.)

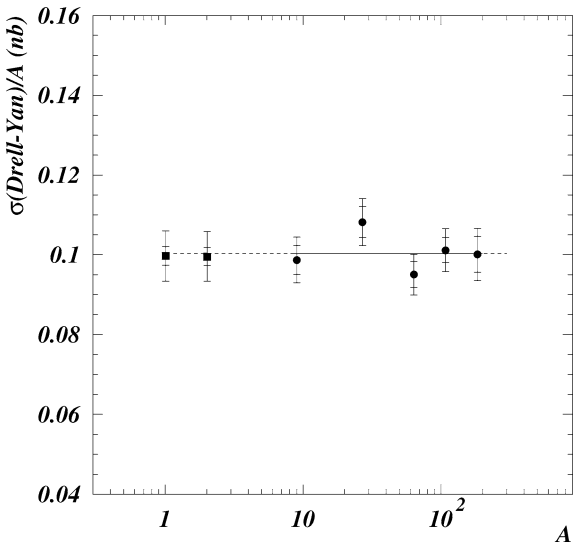

Fig. 3. The isospin corrected Drell–Yan (closed circles) cross-section, relative to the mass region $2.9 < m_{\mu\mu} < 4.5$ GeV/c^2, divided by the mass number A. We have plotted both statistical (inner bars) and statistical plus systematical errors (outer bars). The squares represent the NA51 data on p–p and p–d collisions at 450 GeV. The continuous line shows the result of a fit to the NA50 points, according to the function $\sigma_{\rm DY}^{pA}/A = \text{const}$ ($\chi^2/ndf = 0.74$).

notice that $\sigma_{\rm DY}^{pA}/A$ does not depend on A. To quantify this statement, we have fitted the NA50 data points with the function:

$$\sigma_{\rm DY}^{pA}/A = \sigma_{\rm DY}^{pp} A^{\alpha_{\rm DY}-1} \tag{3}$$

leaving $\sigma_{\rm DY}^{pp}$ and $\alpha_{\rm DY}$ as free parameters. Such a parametrization is commonly used to obtain a rough estimation of the size of nuclear effects for hard processes. We get $\alpha_{\rm DY} = 0.995 \pm 0.016\,(\text{stat.}) \pm 0.019$ (syst.), with $\chi^2/ndf = 1.0$. This result shows that, in our kinematical domain, the Drell–Yan cross-section scales with the number of nucleon–nucleon collisions. We stress that we have chosen the mass interval $2.9 < m_{\mu\mu} < 4.5$ GeV/c^2 for the calculation of the Drell–Yan cross-section in order to be able to compare this set of results with previous measurements performed by NA38 and NA51. Anyway, the choice of a certain mass interval does not affect the results on the A-dependence of the cross-section, since the normalization of the Drell–Yan component is dominated in the fit by the mass region beyond 4 GeV/c^2, where Drell–Yan is the only contribution. In particular we have checked that estimating the cross-section

Table 3
The Drell–Yan cross-sections, divided by the mass number A and multiplied by the isospin correction factors, relative to the mass interval $2.9 < m_{\mu\mu} < 4.5$ GeV/c^2. We quote the statistical and systematical errors separately. The calculated isospin correction factors are also indicated. For p–p and p–d collisions (NA51) the cross-sections have been calculated from the values of $B_{\mu\mu}\sigma_{J/\psi}$ and $B_{\mu\mu}\sigma_{J/\psi}/\sigma_{\rm DY}$ published in Ref. [24]

	$\sigma_{\rm DY}/A$ (pb/A)	Isospin correction
p–Be	98.7 ± 3.7 (stat.) ± 4.4 (syst.)	0.95
p–Al	108.2 ± 3.9 (stat.) ± 4.4 (syst.)	0.95
p–Cu	95.1 ± 3.2 (stat.) ± 3.9 (syst.)	0.95
p–Ag	101.1 ± 3.1 (stat.) ± 4.3 (syst.)	0.95
p–W	100.1 ± 4.5 (stat.) ± 4.7 (syst.)	0.94
p–p (NA51)	99.7 ± 2.4 (stat.) ± 5.9 (syst.)	1.00
p–d (NA51)	99.6 ± 2.3 (stat.) ± 5.8 (syst.)	0.95

by simply counting the events in the mass region $4.3 < m_{\mu\mu} < 8.0$ GeV/c^2 and fitting the results using Eq. (3), we get $\alpha_{\rm DY}^{4.3-8.0} = 0.978 \pm 0.017 \pm 0.019$, a value fully compatible with the one relative to the mass region $2.9 < m_{\mu\mu} < 4.5$ GeV/c^2. Consequently, we conclude that the Drell–Yan process can be used as a reference for the study of nuclear effects on charmonia production. Finally, we stress that in the remaining part of this Letter, when referring to $\sigma_{\rm DY}$, the isospin correction is always included.

In Fig. 4 we plot the cross-section ratios $B_{\mu\mu}\sigma_{J/\psi}/\sigma_{\rm DY}$ and $B'_{\mu\mu}\sigma_{\psi'}/\sigma_{\rm DY}$ as a function of A. Such ratios are particularly useful since, as opposed to absolute cross-sections, they are free from the systematic errors connected with the luminosity measurement and the determination of the various detection efficiencies. Their drawback is the introduction of larger statistical errors because of the relatively small number of Drell–Yan events. Anyway, we find that, with respect to absolute cross-sections, we reduce the total error by 30% on average for results on J/ψ and by 10% for ψ' when considering $B_{\mu\mu}\sigma_{J/\psi}/\sigma_{\rm DY}$ and $B'_{\mu\mu}\sigma_{\psi'}/\sigma_{\rm DY}$. The values are listed in Table 4.

Finally, it is well known that the measured J/ψ yield includes a contribution from χ_c and ψ' radiative decays. While the A-dependence of χ_c production is unknown, we can easily estimate, and remove from the J/ψ sample, the contribution of ψ' decays. Taking into account the values of the branching ratios for the decays $J/\psi \to \mu^+\mu^-$, $\psi' \to \mu^+\mu^-$ and $\psi' \to J/\psi + X$ [20], we obtain that for every measured ψ' we must subtract (3.1 ± 1.1) J/ψ from our data

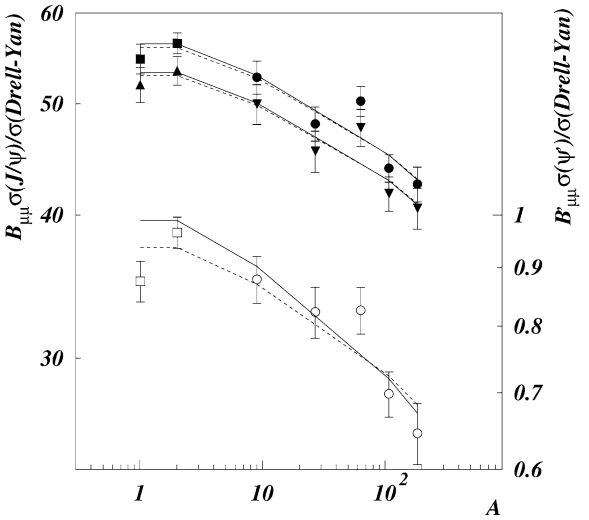

Fig. 4. The ratios $B_{\mu\mu}\sigma_{J/\psi}/\sigma_{\rm DY}$ (closed circles) and $B'_{\mu\mu}\sigma_{\psi'}/\sigma_{\rm DY}$ (open circles) as a function of A. The squares represent the NA51 results. The triangles correspond to the ratio $B_{\mu\mu}\sigma_{J/\psi,{\rm cor}}/\sigma_{\rm DY}$, where the contribution from ψ' decays has been removed from the J/ψ cross-section. The continuous lines represent the result of the Glauber fits to the NA50 data, while the dashed lines correspond to fits which include NA51 points.

Table 4
Ratios of charmonia cross-sections with respect to Drell–Yan. In the last column the J/ψ cross-section has been corrected for the contribution of ψ' decays. For p–p and p–d collisions (NA51) the data on $B_{\mu\mu}\sigma_{J/\psi}/\sigma_{\rm DY}$ have been taken from Ref. [24], while $B'_{\mu\mu}\sigma_{\psi'}/\sigma_{\rm DY}$ has been calculated from the results of Ref. [10] and Ref. [24]

	$B_{\mu\mu}\sigma_{J/\psi}/\sigma_{\rm DY}$	$B'_{\mu\mu}\sigma_{\psi'}/\sigma_{\rm DY}$	$B_{\mu\mu}\sigma_{J/\psi,{\rm cor}}/\sigma_{\rm DY}$
p–Be	52.7 ± 1.7	0.879 ± 0.042	50.0 ± 2.0
p–Al	48.0 ± 1.6	0.823 ± 0.042	45.5 ± 1.9
p–Cu	50.3 ± 1.5	0.826 ± 0.039	47.7 ± 1.8
p–Ag	43.9 ± 1.2	0.698 ± 0.032	41.7 ± 1.4
p–W	42.5 ± 1.5	0.645 ± 0.040	40.5 ± 1.7
p–p (NA51)	54.7 ± 1.6	0.875 ± 0.036	52.0 ± 1.8
p–d (NA51)	56.4 ± 1.2	0.965 ± 0.030	53.4 ± 1.5

sample. The values of $B_{\mu\mu}\sigma_{J/\psi,{\rm cor}}/\sigma_{\rm DY}$, corrected for the contamination from ψ' decays, are plotted in Fig. 4 and included in Table 4.

4. Charmonia absorption

From the experimental results presented in the previous section, it is in principle possible to determine the absorption cross-section in nuclear matter for the J/ψ and ψ' produced in the NA50 kinematical domain. However, although the $c\bar{c}$ production process can be described by perturbative QCD, the hadronization of the heavy quark pair, leading to the formation of a colour-neutral resonance with well-defined quantum numbers, is of non-perturbative nature and occurs on a relatively long time scale. This fact has been experimentally confirmed at positive x_F by the similar A-dependence of J/ψ and ψ' cross-sections [2–5], in spite of their very different size and binding energy. This is a clear indication that in p–A collisions the target nucleons interact with a pre-resonant charmonium state [21]. Therefore, the absorption cross-section for a given observed charmonium state that we can extract from the A-dependence of the production cross-section, corresponds to the value of the interaction cross-section of the evolving $c\bar{c}$ pair in its way through the nucleus.

In this Letter, we use a Glauber approach to determine, from $B_{\mu\mu}\sigma_{J/\psi}/\sigma_{\rm DY}$, $B'_{\mu\mu}\sigma_{\psi'}/\sigma_{\rm DY}$ and $B_{\mu\mu}\sigma_{J/\psi,{\rm cor}}/\sigma_{\rm DY}$, the effective absorption cross-sections $\sigma^{\rm abs}_{J/\psi}$, $\sigma^{\rm abs}_{\psi'}$ and $\sigma^{\rm abs}_{J/\psi,{\rm cor}}$. More in detail, assuming that $\sigma^{pA}_{\rm DY} = A\sigma^{pp}_{\rm DY}$, we fit our experimental data points with the relation [22]:

$$\frac{\sigma^{pA}_i}{\sigma^{pA}_{\rm DY}} = C_i \frac{1}{(A-1)\sigma^{\rm abs}_i} \times \int d^2b \left(1 - e^{-(A-1)T_A(\vec{b})\sigma^{\rm abs}_i}\right), \tag{4}$$

where i represents the process under study (J/ψ, ψ' or J/ψ, cor), $\vec{b}$ is the impact parameter of the p–A collision, and

$$C_i = \frac{\sigma^{pp}_i}{\sigma^{pp}_{\rm DY}}, \qquad T_A(\vec{b}) = \int_{-\infty}^{\infty} dz\, \rho_A(\vec{b}, z), \tag{5}$$

where z is the incident beam direction. We have used the parametrizations of nuclear densities $\rho_A(r)$ from Ref. [23]. The free parameters in the fits are the charmonia absorption cross-sections $\sigma^{\rm abs}_i$ and the normalization constants C_i. The results of the fits are shown in Table 5, and plotted in Fig. 4.

The NA51 experiment has made a high statistics study of J/ψ, ψ' and Drell–Yan production in p–p and p–d collisions at 450 GeV/c, with the same experimental apparatus used by NA50, and in the same

Table 5
Results of the Glauber fit to the ratios $B_{\mu\mu}\sigma_{J/\psi}/\sigma_{\rm DY}$, $B_{\mu\mu}\sigma_{J/\psi,{\rm cor}}/\sigma_{\rm DY}$ and $B'_{\mu\mu}\sigma_{\psi'}/\sigma_{\rm DY}$. The meaning of the normalization constants C is defined in the text. r is the correlation coefficient between $\sigma_{\rm abs}$ and C. For completeness we also quote the results of a fit to the data with the commonly used function $\sigma_i^{pA}/\sigma_{\rm DY}^{pA} = (\sigma_i^{pp}/\sigma_{\rm DY}^{pp})A^{\alpha_i-1}$ ($i = J/\psi$, J/ψ, cor, ψ'). Data sets including the NA51 points have not been fitted since it is known that this parametrization of the absorption effects cannot be applied to low A nuclei when $\sigma_{\rm abs}$ is not negligible [1]

	C	$\sigma_{\rm abs}$ (mb)	χ^2/ndf	r	α	χ^2/ndf
J/ψ	56.4 ± 2.3	4.4 ± 1.0	2.4	0.94	0.933 ± 0.014	2.5
J/ψ (incl. NA51)	55.9 ± 0.9	4.2 ± 0.5	1.6	0.72		
J/ψ, cor	53.5 ± 2.6	4.3 ± 1.2	1.6	0.93	0.934 ± 0.018	1.6
J/ψ, cor (incl. NA51)	52.9 ± 1.1	4.1 ± 0.6	1.0	0.73		
ψ'	0.99 ± 0.05	6.4 ± 1.5	1.5	0.91	0.906 ± 0.022	1.7
ψ' (incl. NA51)	0.94 ± 0.02	5.1 ± 0.8	1.9	0.68		

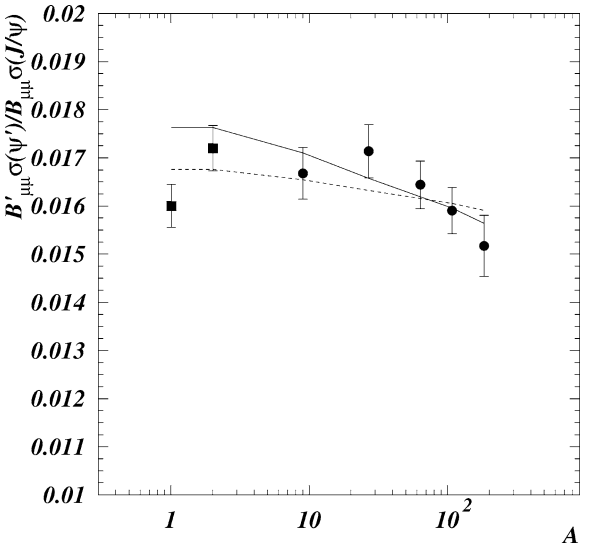

Fig. 5. The ratio $B'_{\mu\mu}\sigma_{\psi'}/B_{\mu\mu}\sigma_{J/\psi}$ as a function of A. The squares represent the NA51 results. The continuous line is the result of the Glauber fit to the NA50 data, while the dashed line corresponds to a fit which includes NA51 points [10].

kinematical region of our p–A data [24]. Therefore, we have also performed a fit of $B_{\mu\mu}\sigma_{J/\psi}/\sigma_{\rm DY}$ including the NA51 points. The results are shown in Table 5 and Fig. 4.

Concerning $\sigma_{J/\psi}^{\rm abs}$ we find that the results for the various fits are compatible. Including p–p and p–d data points, the error on $\sigma_{J/\psi}^{\rm abs}$ and the χ^2/ndf significantly decrease. By removing the ψ' contamination from the J/ψ sample, we obtain a further increase in the quality of the fit. Finally, we observe that when the NA51 points are included, the normalization constants $C_{J/\psi}$, $C_{J/\psi,{\rm cor}}$ are more strongly constrained, leading to a smaller correlation between the fit parameters.

Table 6
The ratios between ψ' and J/ψ cross-sections. For p–p and p–d collisions (NA51) data are taken from Ref. [10]

	$B'_{\mu\mu}\sigma_{\psi'}/B_{\mu\mu}\sigma_{J/\psi}$ (%)
p–Be	1.67 ± 0.05
p–Al	1.71 ± 0.06
p–Cu	1.64 ± 0.05
p–Ag	1.59 ± 0.05
p–W	1.52 ± 0.06
p–p (NA51)	1.60 ± 0.04
p–d (NA51)	1.71 ± 0.04

Concerning the ψ', we find an absorption cross-section slightly higher than that of the J/ψ, confirming the observation of E866, made at 800 GeV/c incident energy [5]. By directly fitting with our Glauber approach the $B'_{\mu\mu}\sigma_{\psi'}/B_{\mu\mu}\sigma_{J/\psi}$ ratios as a function of A, we estimate $\Delta\sigma = \sigma_{\psi'}^{\rm abs} - \sigma_{J/\psi}^{\rm abs}$. In Fig. 5 and Table 6 we show $B'_{\mu\mu}\sigma_{\psi'}/B_{\mu\mu}\sigma_{J/\psi}$ together with the results of the fit. We find $\Delta\sigma = (2.2 \pm 1.0)$ mb when fitting the NA50 points, and $\Delta\sigma = (0.9 \pm 0.6)$ mb when NA51 results are included. The accuracy on the determination of $\Delta\sigma$ is clearly dominated by the number of detected ψ'. By fitting the NA50 points on the cross-sections ratio with the power law function $B'_{\mu\mu}\sigma_{\psi'}^{pA}/B_{\mu\mu}\sigma_{J/\psi}^{pA} = B'_{\mu\mu}\sigma_{\psi'}^{pp}/B_{\mu\mu}\sigma_{J/\psi}^{pp} \cdot A^{\alpha_{\psi'}-\alpha_{J/\psi}}$ we get $\Delta\alpha = \alpha_{\psi'} - \alpha_{J/\psi} = -0.028 \pm 0.015$. Finally, very high statistics data (about 5 times the present sample) have been recently collected by NA50 and will allow a significant increase in the accuracy of this measurement, as well as the study of $\sigma_{\rm abs}^{\psi'}$ in various bins of y and p_T.

Coming back to the J/ψ, the estimate of $\sigma_{J/\psi}^{\rm abs}$ in p–A interactions provides a useful reference for the study of J/ψ suppression in nucleus–nucleus collisions, relevant for the study of deconfinement. In the remaining part of this section, we will compare the absorption cross-section extracted from p–A data with the same quantity obtained for S–U collisions. More in detail, $\sigma_{J/\psi}^{\rm abs}$ can be estimated from the data on the ratio $B_{\mu\mu}\sigma_{J/\psi}/\sigma_{\rm DY}$, measured for various centrality bins by the NA38 Collaboration [25]. Obviously, a larger J/ψ absorption cross-section for S–U with respect to p–A would imply the onset of an additional source of J/ψ suppression, possibly due to the interaction of the J/ψ with comoving secondary hadrons, or to the production of a deconfined phase. We have adopted, for the analysis of S–U data, the same Glauber approach used for p–A, generalized in order to take into account the centrality of the collision [26]. We recall that the NA38 data were taken at 200 GeV/nucleon incident energy, in the kinematical window $0 < y_{\rm cm} < 1$, $-0.5 < \cos\theta_{\rm CS} < 0.5$ and that the isospin correction factor applied to the Drell–Yan cross-section was 0.99 [10].

By fitting the S–U points we get $\sigma_{J/\psi}^{\rm abs,SU} = (7.1 \pm 3.0)$ mb, a value which, although larger, is compatible within errors with $\sigma_{J/\psi}^{\rm abs,\,pA}$. The large uncertainty on $\sigma_{J/\psi}^{\rm abs,SU}$ is due to the large relative error on the S–U data and to the very strong correlation between the fit parameters. When the ψ' contamination is removed, using the S–U data on $B'_{\mu\mu}\sigma_{\psi'}/\sigma_{\rm DY}$ published in Ref. [25], one gets $\sigma_{J/\psi,{\rm cor}}^{\rm abs,SU} = (6.3 \pm 2.9)$ mb. The decrease in the absorption cross-section can be easily explained by considering that in S–U collisions the ψ' is much more absorbed than the J/ψ, a fact commonly interpreted as due to the breaking of the loosely bound ψ' state in interactions with comoving hadrons produced in the collision. As a consequence, the contamination of ψ' decays in the J/ψ sample is less important for central collisions with respect to peripheral, leading, after subtraction, to a flattening of $B_{\mu\mu}\sigma_{J/\psi,{\rm cor}}/\sigma_{\rm DY}$ versus centrality. The S–U points, together with the results of the fits, are plotted in Fig. 6 as a function of the measured neutral transverse energy $E_{\rm T}$, measured by NA38 in the pseudorapidity range $1.7 < \eta < 4.1$. The values of the fit parameters can be found in Table 7.

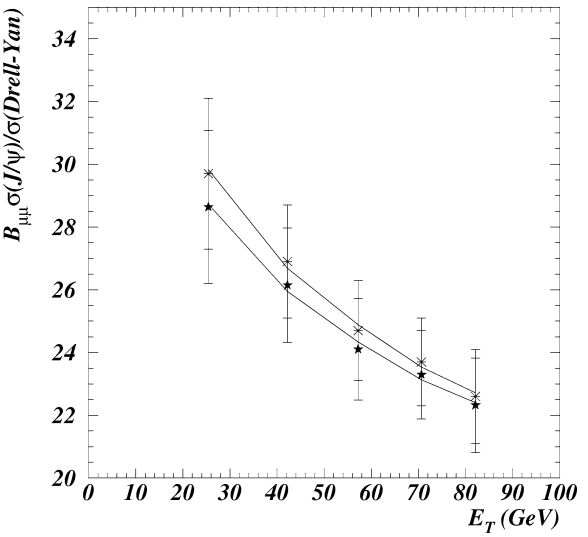

Fig. 6. The ratios $B_{\mu\mu}\sigma_{J/\psi}/\sigma_{\rm DY}$ (asterisks) and $B_{\mu\mu}\sigma_{J/\psi,{\rm cor}}/\sigma_{\rm DY}$ (stars) as a function of the measured neutral transverse energy $E_{\rm T}$, for S–U collisions. The lines represent the results of the Glauber fits to the data.

Since the J/ψ absorption cross-sections in p–A and S–U have been found to be compatible, we have performed a simultaneous fit of p–A and S–U points, in order to check if the data can be satisfactorily described by a common value of the absorption cross-section. We take into account that the S–U data sample was collected at a different energy and with a slightly different rapidity coverage with respect to p–A, by introducing as a free parameter in the fit a rescaling factor between the normalizations of the p–A and S–U points. From the E866 results [5], which show a flat behaviour of $\sigma_{J/\psi}^{\rm abs}$ around $x_F = 0$, we do not expect a variation of $\sigma_{J/\psi}^{\rm abs}$ due to the slightly different $y_{\rm cm}$ coverage of the two sets of data. Having verified that ψ' decay contamination plays a significant role in determining $\sigma_{J/\psi}^{\rm abs}$ for S–U collisions, we have performed the simultaneous fit to p–A and S–U points after having removed this contamination. The NA51 points have been included in the fit, since we have seen above that in p–A collisions they help in reducing the correlation between the parameters, without significantly affecting the value of $\sigma_{J/\psi}^{\rm abs}$. We find that p–A and S–U points can be well described ($\chi^2/ndf = 0.6$) with the value of the absorption cross-section $\sigma_{J/\psi,{\rm cor}}^{\rm abs,\,pA+SU} = (4.3 \pm 0.6)$ mb. The values of the fit parameters are summarized in

Table 7
Results of the Glauber fit to the ratios $B_{\mu\mu}\sigma_{J/\psi}/\sigma_{\rm DY}$ and $B_{\mu\mu}\sigma_{J/\psi,{\rm cor}}/\sigma_{\rm DY}$ for S–U collisions. We also show the results of the simultaneous fits to p–A and S–U points (see text for details)

	C	$\sigma_{\rm abs}$ (mb)	χ^2/ndf	r
S–U	52.7 ± 14.9	7.1 ± 3.0	0.02	0.998
S–U, cor	48.0 ± 13.9	6.3 ± 2.9	0.02	0.994
p–A (including NA51) + p–W, 200 GeV + p–U, 200 GeV + S–U, cor	53.2 ± 1.0	4.3 ± 0.6	0.6	
p–A (including NA51) + p–W, 200 GeV + p–U, 200 GeV + S–U	56.2 ± 0.8	4.4 ± 0.5	1.0	

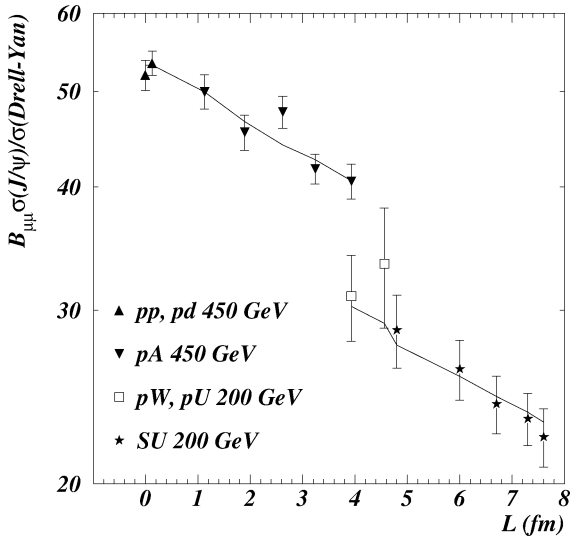

Fig. 7. The ratios $B_{\mu\mu}\sigma_{J/\psi,{\rm cor}}/\sigma_{\rm DY}$, for p–A and at 200 GeV/nucleon for S–U collisions, plotted as a function of the L variable, defined in the text. The line represents the result of the Glauber fit. The p–A data include the NA51 results, the p–A values presented in this Letter (triangles) and the p–W and p–U points (open squares) measured at 200 GeV by the NA38 Collaboration [10].

Table 7. In Fig. 7 we present the p–A and S–U points together with the result of the fit. In order to show proton–nucleus and nucleus–nucleus data on a single plot, we have used the L variable, defined as the average thickness of nuclear matter seen by the $c\bar{c}$ pair in its way through projectile and target nuclei, and calculated in the framework of the Glauber model.

From the fit, we get the value 0.75 ± 0.04 for the ratio

$$F_{J/\psi/{\rm DY}} = \frac{F_{J/\psi}}{F_{\rm DY}} = \frac{\sigma^{pp}_{J/\psi,200}/\sigma^{pp}_{J/\psi,450}}{\sigma^{pp}_{{\rm DY},200}/\sigma^{pp}_{{\rm DY},450}} \qquad (6)$$

between the normalizations of the points at the two different energies. We have compared this value with three different estimates of the same quantity. In what concerns J/ψ production, we have used:

- a commonly used parameterization of the $\sqrt{s}$ and x_F dependence of the production cross-sections [27];
- a NLO QCD calculation [28];
- a simultaneous Glauber fit to our p–A data on absolute J/ψ cross-sections at 450 GeV/c and to available p–A data at 200 GeV/c from the NA3 and NA38 Collaborations [2,10].

Concerning Drell–Yan we have used a leading order calculation, with the MRS (A) low Q^2 $\overline{\rm MS}$ set of parton distribution functions. The calculated $F_{J/\psi}$, $F_{\rm DY}$ and $F_{J/\psi/{\rm DY}}$ values are shown in Table 8. We see that the calculated $F_{J/\psi/{\rm DY}}$ values are in fair agreement with our experimental estimate. For completeness we also quote in Table 8 the factorization of the $F_{J/\psi}$, $F_{\rm DY}$ and $F_{J/\psi/{\rm DY}}$ ratios into "energy" and "rapidity" components. The first takes into account the $\sqrt{s}$ dependence of the J/ψ and Drell–Yan cross-sections and the second the different rapidity coverage of our apparatus at the two energies.

Finally, to ease the comparison with previous estimates of $\sigma^{\rm abs}_{J/\psi}$ which did not include neither the p–A results presented in this Letter nor the correction for the contamination from ψ' decays, we show in Fig. 8 the results of the simultaneous fit to p–A and S–U data points, relative to the $B_{\mu\mu}\sigma_{J/\psi}/\sigma_{\rm DY}$ values.

5. Conclusions

We have measured J/ψ, ψ' and Drell–Yan production at central rapidity in p–A collisions at 450 GeV/c.

Table 8
Compilation of the calculated ratios $F_{J/\psi}$ and $F_{\rm DY}$ between the production cross sections at 200 and 450 GeV incident energy for p–p collisions. F_i^E is the ratio $\sigma_{i,200}^{pp}(-0.4 < y_{\rm cm} < 0.6)/\sigma_{i,450}^{pp}(-0.4 < y_{\rm cm} < 0.6)$, F_i^y is the ratio $\sigma_{i,200}^{pp}(0 < y_{\rm cm} < 1)/\sigma_{i,200}^{pp}(-0.4 < y_{\rm cm} < 0.6)$, while F_i is the product of the two quantities for the process i ($i = J/\psi$, DY). The ratio $F_{J/\psi/\rm DY} = F_{J/\psi}/F_{\rm DY}$ is also shown. See text for details on the three calculations of $F_{J/\psi}$

$\sigma_{J/\psi}$	$F^E_{J/\psi}$	$F^y_{J/\psi}$	$F_{J/\psi}$
Schuler [27]	0.55 ± 0.03	0.76 ± 0.10	0.42 ± 0.07
QCD NLO [28]	0.46	0.82	0.38
NA3, NA38, NA50, NA51 [2,10]			0.32 ± 0.03

$\sigma_{\rm DY}$	$F^E_{\rm DY}$	$F^y_{\rm DY}$	$F_{\rm DY}$
LO	0.53	0.93	0.49

$\sigma_{J/\psi}/\sigma_{\rm DY}$	$F^E_{J/\psi/\rm DY}$	$F^y_{J/\psi/\rm DY}$	$F_{J/\psi/\rm DY}$
Schuler [27]	1.04 ± 0.06	0.82 ± 0.11	0.85 ± 0.14
QCD NLO [28]	0.87	0.88	0.77
NA3, NA38, NA50, NA51 [2,10]			0.65 ± 0.05

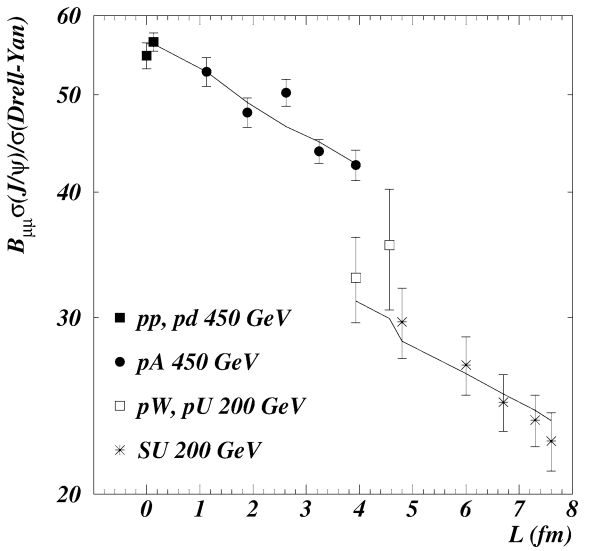

Fig. 8. Same as previous figure, without correcting the J/ψ yields for the ψ' feed-down contribution.

The Drell–Yan cross-section has been found to scale with the number of nucleon–nucleon collisions. Using the Glauber model, we have calculated from our data the absorption cross-section $\sigma^{\rm abs}_{J/\psi}$ and $\sigma^{\rm abs}_{\psi'}$ for charmonia in nuclear matter, fitting the ratios $B_{\mu\mu}\sigma_{J/\psi}/\sigma_{\rm DY}$ and $B'_{\mu\mu}\sigma_{\psi'}/\sigma_{\rm DY}$ for various target nuclei, from $A = 1$ to $A = 184$. After subtracting the contribution of ψ' decays to the J/ψ yield, we find $\sigma^{\rm abs}_{J/\psi,\rm cor} = (4.1 \pm 0.6)$ mb. We have also performed a simultaneous fit of $B_{\mu\mu}\sigma_{J/\psi}/\sigma_{\rm DY}$ for p–A and S–U collisions, using the S–U data published by NA38. We find that the two sets of data can be well described by a single value of the absorption cross-section. In particular, we get $\sigma^{\rm abs}_{J/\psi} = (4.4 \pm 0.5)$ mb and, when the contamination from ψ' decays is subtracted, $\sigma^{\rm abs}_{J/\psi,\rm cor} = (4.3 \pm 0.6)$ mb. These results show that the sulphur–uranium data can be explained without invoking J/ψ suppression mechanisms different from the ones already taking place in proton–nucleus collisions.

References

[1] See: R. Vogt, Phys. Rep. 310 (1999) 197, and references therein.
[2] NA3 Collaboration, J. Badier, et al., Z. Phys. C 20 (1983) 101.
[3] E772 Collaboration, D.M. Alde, et al., Phys. Rev. Lett. 66 (1991) 133.
[4] NA38 Collaboration, M.C. Abreu, et al., Phys. Lett. B 444 (1998) 516.
[5] E866 Collaboration, M.J. Leitch, et al., Phys. Rev. Lett. 84 (2000) 3256.
[6] T. Matsui, H. Satz, Phys. Lett. B 178 (1986) 416.
[7] NA50 Collaboration, M.C. Abreu, et al., Phys. Lett. B 410 (1997) 337.
[8] NA50 Collaboration, M.C. Abreu, et al., Phys. Lett. B 450 (1999) 456.
[9] NA50 Collaboration, M.C. Abreu, et al., Phys. Lett. B 477 (2000) 28.
[10] NA38 Collaboration, M.C. Abreu, et al., Phys. Lett. B 466 (1999) 408.
[11] P. Cortese, PhD thesis, Università di Torino, 2000.

[12] NA50 Collaboration, E. Scomparin, et al., Nucl. Phys. A 698 (2002) 543c.
[13] R. Shahoyan, PhD thesis, Universidade Técnica de Lisboa, 2001.
[14] NA50 Collaboration, M.C. Abreu, et al., Phys. Lett. B 410 (1997) 327.
[15] L. Anderson, et al., Nucl. Instrum. Methods 223 (1984) 26.
[16] NA50 Collaboration, M.C. Abreu, et al., Eur. Phys. J. C 14 (2000) 443.
[17] C. Lourenço, PhD thesis, Universidade Técnica de Lisboa, 1995.
[18] T. Sjostrand, Comput. Phys. Commun. 82 (1994) 74.
[19] A.D. Martin, et al., Phys. Rev. D 51 (1995) 4756.
[20] Particle Data Group, D.E. Groom, et al., Eur. Phys. J. C 15 (2000) 1.
[21] D. Kharzeev, H. Satz, Phys. Lett. B 366 (1996) 316.
[22] J.P. Blaizot, J.Y. Ollitrault, Phys. Rev. Lett. 77 (1996) 1703.
[23] H. DeVries, et al., At. Data Nucl. Data Tables 36 (1987) 495.
[24] NA51 Collaboration, M.C. Abreu, et al., Phys. Lett. B 438 (1998) 35.
[25] NA38 Collaboration, M.C. Abreu, et al., Phys. Lett. B 449 (1999) 128.
[26] D. Kharzeev, et al., Z. Phys. C 74 (1997) 307.
[27] G.A. Schuler, Habilitationsschrift, Univ. Hamburg, 1994, CERN-TH-7170-94.
[28] R. Vogt, private communication.